Estuaries and Coasts (2025) 48:63
https://doi.org/10.1007/s12237-025-01494-4

Carbonate and Nutrient Dynamics in a Mississippi River Influenced Eutrophic Estuary

Songjie He[1,2] · Sean Gordon[1,3] · Kanchan Maiti[1]

Received: 17 July 2024 / Revised: 16 January 2025 / Accepted: 27 January 2025

Abstract
There is limited information on how the nutrient and freshwater input affects water column carbonate chemistry in the estuaries along the northern Gulf of Mexico. In this study, we assess the seasonal and spatial variability in carbonate chemistry in the Barataria Basin, a eutrophic estuary adjacent to the mouth of the Mississippi River. Eleven stations were sampled along a salinity gradient during the winter (January), spring (April), summer (July), and fall (October) of 2021. Surface and bottom water samples were collected for the analyses of dissolved inorganic carbon (DIC); total alkalinity (TA); and nitrite plus nitrate ($NO_2 + NO_3$), phosphate (PO_4), and dissolved silica (SiO_4). Dissolved CO_2 (pCO_2) was measured in the surface water. Seasonal surface DIC and TA values ranged from 1553 to 2582 µmol kg^{-1} and 1217 to 2217 µmol kg^{-1}, respectively. DIC and TA varied seasonally and showed an increasing trend from fresh stations to saline stations. The highest DIC and TA values were observed during the fall season, likely due to the increased contribution of DIC and TA from adjacent marshes as a result of enhanced porewater exchange. In contrast to DIC and TA, pCO_2 decreased with the increase of salinity. The seasonal and spatial patterns in carbonate chemistry could not be explained solely by physical mixing and reflected complex interactions between biogeochemical processes driven by nutrient supply and temperature as well as tidal flushing and material exchanges with adjacent marshes.

Keywords Carbonate · Nutrients · Barataria Estuary · Mississippi River · Gulf of Mexico

Introduction

Carbon dioxide emissions have increased by more than 40% since industrialization with roughly a third of those emissions being absorbed into the world's oceans (Cai et al., 2021; IPCC, 2023; Sabine et al., 2004). While the absorption of CO_2 by oceans has reduced the net increase in atmospheric CO_2, it has also resulted in unprecedented surface ocean acidification via production of carbonic acid (H_2CO_3). This process has increased the hydrogen ion concentration ($[H^+]$) in surface ocean water by ~31% and decreased pH by 0.12 units since preindustrial times (Sunda & Cai, 2012). Although there is global evidence of ocean acidification in open ocean waters (Bates et al., 2014; Osborne et al., 2022), pH declines in estuaries have largely been attributed to eutrophication (Abril et al., 2004; Sarma et al., 2011). Understanding of the critical roles the estuarine inorganic carbon system (CO_2, HCO_3^-, CO_3^{2-}) and nutrients play in the global carbon cycle can provide insight on acidifying conditions in coastal waters.

In addition to rising atmospheric CO_2, other processes can also increasingly acidify coastal waters and estuaries, which are interconnected with carbonate chemistry in these systems (Cai et al., 2021; Kelly et al., 2011; Sippo et al., 2016). Approximately 40% of the world population lives within 100 km of a coastline, making these regions subject to a suite of anthropogenic stressors including intense nutrient loading (de Jonge et al., 2002). Eutrophication, which is caused by excessive nutrients, promotes algal productivity, and the subsequent microbial consumption of this organic

Communicated by Paul A. Montagna

✉ Kanchan Maiti
kmaiti@lsu.edu

[1] Department of Oceanography and Coastal Sciences, Louisiana State University, Baton Rouge, LA, USA

[2] Division of Coastal Sciences, School of Ocean Science and Engineering, The University of Southern Mississippi, Ocean Springs, MS, USA

[3] Collegiate High School, Northwest Florida State College, Niceville, FL, USA

Published online: 15 February 2025

matter reduces oxygen levels and can promote hypoxia. Another often overlooked consequence of this is the increase in water column CO_2 production due to enhanced respiration that forms carbonic acid (H_2CO_3), which then dissociates into bicarbonate ions (HCO_3^-), carbonate ions (CO_3^{2-}), and hydrogen ions (H^+) that cause changes in carbonate chemistry (Feely et al., 2010; Cai et al., 2010). A better understanding of how carbonate chemistry varies seasonally and affects coastal systems is of major importance due to the increased anthropogenic activity associated with coastal areas. Furthermore, model studies do not always include data in shallower coastal regions due to the dynamic and ever-changing environmental parameters that govern these areas.

The Northern Gulf of Mexico (NGOM) is a sink of atmospheric CO_2 (Xue et al., 2016); however, due to high temperature and alkalinity, it is regarded as a well-buffered coastal system. The Louisiana shelf, an area of ecological and economic importance in the NGOM, receives nutrients from the Mississippi-Atchafalaya River system that led to eutrophication (Peyronnin et al., 2017; Rabalais et al., 2002; White et al., 2019). The Mississippi River system concludes in coastal Louisiana where it forms a massive oxygen-depleted zone in the NGOM during summer and early fall (Rabalais et al., 2002). The work done on this hypoxic zone, 1970 to present, has a major focus on how increased nutrient loading coming from the Mississippi-Atchafalaya River system causes increased organismal growth and respiration that influences the severity of hypoxia on the continental shelf and surrounding waters (Huang et al., 2021; Quiñones-Rivera et al., 2022; Rabalais et al., 2002; Wang et al., 2020). Louisiana shelf is a well-studied area, in terms of eutrophication and hypoxia. There is, however, limited information on how these processes indirectly affect water column carbonate chemistry, with most studies restricted to the hypoxia zone (Cai et al., 2011; Hu et al., 2017; Huang et al., 2021; Murrell et al., 2013; Platon et al., 2005; Quiñones-Rivera et al., 2022; Wang et al., 2020) and none in the estuaries. Furthermore, seasonality in estuarine dissolved inorganic carbon (DIC) and alkalinity can have a pronounced impact on the buffering capacity, carbonate speciation, and pH of coastal waters (Song et al., 2020; Wang et al., 2016). However, inorganic carbon data for most estuarine systems are insufficient to define spatial and seasonal heterogeneity, which is necessary for establishing baseline acidification and buffering information from which trends can be evaluated. This information gap is a serious obstacle for resource management in these economically and socially valuable systems. Information regarding carbonate parameters of estuaries, particularly those most vulnerable today, could provide critical insight on future issues both economic and ecological. In this study, we examine the spatial and seasonal variabilities of carbonate and nutrient data along a salinity gradient of 0–29 in a eutrophic estuary — the Barataria Basin in Louisiana and evaluate the factors governing the spatiotemporal trends on a seasonal scale.

Methods

Study Area

Barataria Basin is one of the most productive estuarine systems in the northern Gulf of Mexico (Turner et al., 2019; Vargas-Lopez et al., 2021) located south of New Orleans, Louisiana (Fig. 1). It is a ~ 6000 km^2 basin that stretches from the mainstream of the Mississippi River to the abandoned Bayou Lafourche distributary (Anderson et al., 2020; FitzGerald et al., 2004). The northernmost part of the basin is made up of three lakes varying in size and level of eutrophication: hypereutrophic waters in Lac des Allemands, moderate eutrophic levels in Lake Cataouatche, and the least eutrophic of the lakes being Lake Salvador (Ren et al., 2020; Turner et al., 2019). The southernmost part of Barataria Basin is mesotrophic and dominated by marsh habitats that are influenced by the tropic diurnal tide of roughly 0.35 m at the coastline, which decreases significantly along the salinity gradient (Das et al., 2012; Day et al., 2020). The Barataria Bay is bar-built with four tidal passes (Barataria, Caminada, Abel, and Quatre Bayou) to the Gulf of Mexico with an average depth of ~ 2 m. The residence time of water in the bay ranges from 13 to 19 days (Li et al., 2011, 2021).

The hydrodynamics in the Barataria Basin are complex and are affected by river discharge, tides, waves, cold fronts, tropical storms, and hurricanes (Das et al., 2012; Sorourian et al., 2020). Salinities range from near zero in the upper reaches of the estuary to about 25 in the southernmost section of the estuary. Freshwater input into the basin is limited and has several sources — episodic rainfall; stream runoff; seepage from the Mississippi River channel, Mississippi River siphons (West Pointe a la Hache and Naomi); the Gulf Intracoastal Waterway; and the Davis Pond Freshwater Diversion (DPD) to the north, which was designed to push back the saltwater intrusion and has a maximum design discharge capacity of 300 $m^3\ s^{-1}$ (Das et al., 2012; Jung et al., 2023). The DPD diverts freshwater and dissolved nutrients from the Mississippi River directly into the basin from the northern side, which then moves southward into the estuary (Day et al., 2020). Advection of Mississippi River water to the eastern part of lower Barataria Bay can happen during flood period as the clockwise gyre in the Louisiana Bight moves Mississippi River fresh water towards the shoreline (Cui et al., 2018; Payandeh et al., 2019). This region is currently undergoing one of the highest levels of wetland loss in the country (Couvillion et al., 2017), which supplies additional soil-bound organic matter into the basin further fueling respiration in the water column.

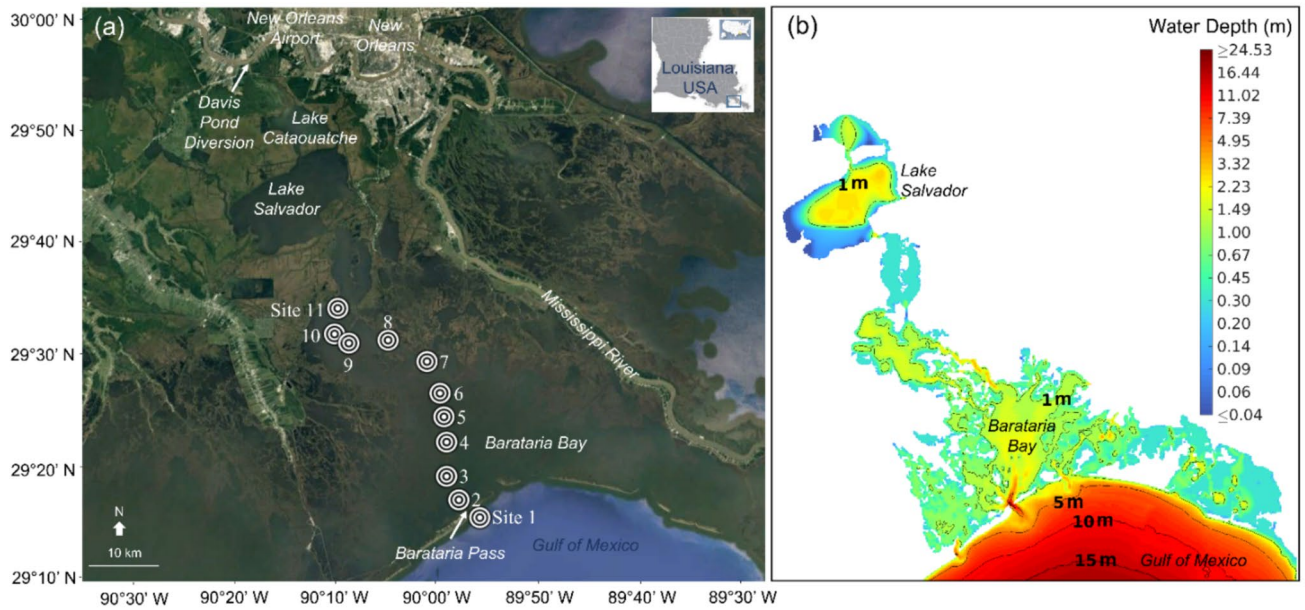

Fig. 1 **a** Sampling stations (sites 1 to 11) in the Barataria Basin, Louisiana, located in the north-central Gulf of Mexico, just to the west of the Mississippi River; **b** bathymetry of the Barataria Basin (adapted from Ou et al., 2020)

The region can be characterized as subtropical with long, hot, and humid summers and generally short, mild winters. The average monthly temperature ranged from 12.3 °C in February 2021 to 28.9 °C in August 2021, with a mean of 21.8 °C for the 1-year study period (January to December 2021). The monthly precipitation totals ranged from 13.2 mm in November 2021 to 326.4 mm in April 2021, with a monthly mean of 180.7 mm for the 12 months (Fig. 2, NOAA National Centers for Environmental Information site: New Orleans Airport, LA, USA).

Field Sampling

Seasonal sampling in the Barataria Basin was carried out four times during winter (January 18th), spring (April 20th), summer (July 27th), and fall (October 26th) of 2021 to capture temporal variability associated with freshwater input and biogeochemical processes. All field campaigns were conducted using a small motorboat during the daytime. During each season, samples were collected from 11 stations along a south to north transect in the Barataria Basin to capture the salinity gradient (Fig. 1). The sampling stations along this transect were numbered so as to increase progressively from south to north with station 1 being located at the main inlet of the bay called the Barataria Pass (Fig. 1).

During each trip, water quality parameters, such as temperature, salinity, and dissolved oxygen (DO) concentration, were measured in situ using a YSI handheld meter (YSI professional plus; Yellow Springs, OH, USA). DO was also measured using an optode-based DO datalogger (PME miniDOT, California, USA) to cross validate the DO measured using the YSI. DO saturations were calculated using temperature, salinity, and the equation and parameters from Garcia & Gordon, 1992. DO saturation rates (DO% = measured DO concentration / DO saturation) are presented to exclude seasonal temperature influence on DO.

Surface water partial pressure of dissolved CO_2 (pCO_2), defined as the CO_2 in 100% water-saturated air that is in equilibrium with the water, was measured using a CO_2-Pro™ CV Submersible pCO_2 Sensor (Pro-oceanus, Nova Scotia Canada) through a flow-through system by passing surface water at constant flow rate of 2–2.5 L s^{-1}, which resulted in continuous water pCO_2 measurements every 10 s during the sampling trips. To make the comparison with other parameters easier, we extracted and averaged the pCO_2 measurements at each site when the boat was stationary. During the July 27, 2021 field trip, we were not able to collect any pCO_2 data due to sensor malfunction. Therefore, a separate trip on July 11, 2022, was made to represent summer pCO_2 data.

Discrete water samples were collected at each station from a consistent depth of 0.5 m below the surface and 0.5 m from the bottom for analysis of dissolved inorganic carbon (DIC), TA, and nutrients, such as dissolved silica (SiO_4), phosphate (PO_4), and nitrite plus nitrate ($NO_2 + NO_3$). Water samples for DIC and TA were passed through a 0.45-µm glass fiber syringe filter and collected without headspace into air-tight 40-mL or 10-mL glass vials, by filling from the bottom and allowing overflow of at least the volume of the vial to minimize atmospheric contamination (Anderson et al., 2020; He et al., 2022). DIC and TA samples were

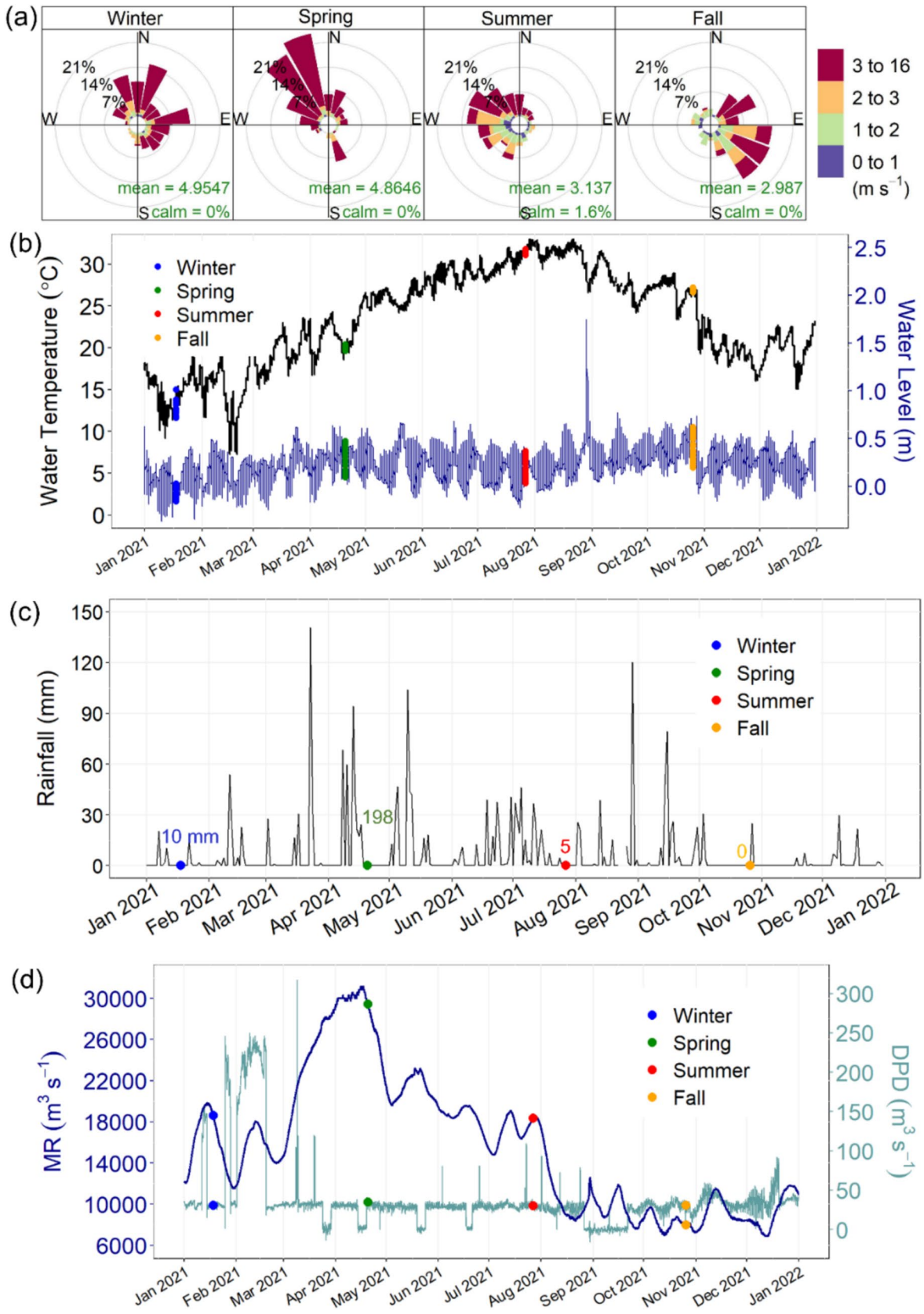
(a)
Winter
Spring
Summer
Fall
N
W
E
S
21%
14%
7%
mean = 4.9547
calm = 0%
mean = 4.8646
calm = 0%
mean = 3.137
calm = 1.6%
mean = 2.987
calm = 0%
3 to 16
2 to 3
1 to 2
0 to 1
(m s -1)
(b)
Water Temperature (°C)
Water Level (m)
Winter
Spring
Summer
Fall
Jan 2021
Feb 2021
Mar 2021
Apr 2021
May 2021
Jun 2021
Jul 2021
Aug 2021
Sep 2021
Oct 2021
Nov 2021
Dec 2021
Jan 2022
(c)
Rainfall (mm)
10 mm
198
5
0
(d)
MR (m3 s-1)
DPD (m3 s-1)

◂**Fig. 2** Environmental parameters in the Barataria Basin, Louisiana: **a** wind at Grand Isle for the week leading up to the sampling days, including the sampling days; **b** water temperature and water level at Grand Isle in 2021, with the temperature and water on sampling days highlighted; **c** rainfall at the New Orleans airport in 2021 with the rainfall on sampling days highlighted, and the cumulative rainfall of the pre-sampling week listed; **d** discharges of the Mississippi River (MR) and Davis Pond Diversion (DPD), with the discharges on sampling days highlighted

preserved with a 20-µL saturated mercuric chloride ($HgCl_2$) solution. Water samples for DIC and TA were transported to the laboratory on ice and stored at 5 °C until analysis. Water samples for nutrients were passed through 0.45-mm glass fiber syringe filters and collected into 20-mL acid-cleaned plastic vials. The nutrient samples were stored on ice and stored in a freezer until analysis.

Lab Analysis

DIC analysis was carried out following the standard protocol associated with the semi-automated system Apollo SciTech AS-C5 Dissolved Inorganic Carbon Analyzer (Newark, DE, USA). This is done by acidifying 1 mL of sample with phosphoric acid, which then converts all carbon forms into carbon dioxide. An infrared CO_2 detector then quantifies the extracted CO_2 from the sample with high precision of < 1% (Cai et al., 1998). The standard curves used for calculating DIC were made using certified reference material (CRM batch 187; DIC = 2002.85 ± 0.50 µmol/kg; Dickson, 2010).

TA measurements were carried out following the Gran titration method (Gran, 1952) using the semi-automated system Apollo SciTech AS-ALK2 Total Alkalinity Titrator (Newark, DE, USA). The precision of this method is less than 1%, and the analyses were carried out at a controlled temperature of 25 °C. The titrator was calibrated using the certified reference material (CRM batch 180; TA = 2224.47 ± 0.56 µmol/kg; Dickson, 2010). Please note that this alkalinity measurement may include the contribution from organic alkalinity (Cai et al., 1998). A recent study of a salt marsh in the northeast USA found organic alkalinity to contribute 0.9–4.3% of TA (Song et al., 2020).

Dissolved nutrient analysis was conducted to determine the concentrations of SiO_4, PO_4, and $NO_2 + NO_3$ using a Cary 60 UV–VIS spectrophotometer following standard protocols outlined in EPA method 366.0, EPA method 365.1, and Schnetger & Lehners, 2014, respectively. Briefly, SiO_4 samples were combined with an ammonium molybdate reagent then mixed with a reducing reagent, which is a mixture of metol-sulfite, oxalic acid, and sulfuric acid, to produce a blue color, the absorbance of which is measured spectrophotometrically. Sodium fluorosilicate was used as the standard for SiO_4 analysis. Dissolved PO_4 samples react with ammonium molybdate and antimony potassium tartrate in an acid medium to form an antimony-phospho-molybdate complex. This complex is reduced to an intensely blue-colored complex by ascorbic acid. Potassium dihydrogen phosphate was used as the standard for PO_4 analysis. Dissolved $NO_2 + NO_3$ samples were mixed with vanadium(III) chloride, N-1-naphthylethylenediamine dihydrochloride, and sulfanilamide solutions. The mixtures were then incubated at 45 °C for 60 min. Absorbance of the incubated samples was then measured at a 540-nm wavelength. Potassium nitrate was the standard used for $NO_2 + NO_3$ analysis.

Data Analysis

Statistical analyses were performed using R statistical packages. All statistical analyses were evaluated at 0.05 levels of significance. The effect of temperature on aqueous pCO_2 is primarily the manifestation of changes in the solubility of CO_2 gas in water (Takahashi et al. 1993). The temperature dependence of pCO_2 in seawater has been described by various authors (Takahashi et al. 1993; Jiang et al., 2008). Seasonal variability in pCO_2 reflects air–water exchange, biological processes, and temperature. Thus, a direct comparison of pCO_2 between seasons must account for any temperature effect. The seasonal variability of surface-water pCO_2 due to temperature variations was removed using the seacarb package in R by converting the measured partial pressure of CO_2 to the fugacity of CO_2, accounting for temperature and pressure, which also changed the unit of pCO_2 from ppm to µatm. All CO_2 data presented in this study are temperature-normalized.

Shapiro–Wilk tests of normality were performed for all environmental parameters as well as carbon and nutrient concentrations using the shapiro.test function in the dplyr package in R. Due to the non-normality of most of the parameters, nonparametric Kruskal–Wallis rank sum tests (kruskal.test function in the dplyr package) were used to evaluate differences between surface and bottom and between seasons. Multiple comparisons of treatments (seasons, surface, and bottom) were made using the HSD.test function by means of Tukey's test, and letters were assigned based on the results (different letter if a statistical difference was found and vice versa).

Results

Spatiotemporal Variations of Environmental Parameters

The Barataria Basin showed large spatial variability in surface salinity ranging from a salinity of 28.5 at the bottom of the southernmost station near the Barataria Pass (site 1) to near zero salinities at the northernmost stations indicating

more dominant influence from the NGOM for the lower Barataria Basin (sites 1–5) than the upper Barataria Basin (sites 6–11) (Fig. 3). The largest surface salinity gradient was observed during the fall when it varied from 23.2 at site 1 to 2.9 at site 11. In contrast, the spring surface salinity was only 16 at site 1 and 0.1 at site 11. The surface salinity distribution was similar during winter and summer of 2021 varying from 20.9 to 0.7 and from 17.8 to 1.5, respectively. The bottom salinity distribution closely followed the surface salinity and tended to be slightly higher at most stations during all seasons, with winter 2021 having the largest surface-bottom stratification (Fig. 3; Table 1). Average salinity was observed to be highest in the fall (14.3) and lowest in the spring (4.6). The low salinities during the spring sampling coincided with strong winds from the north, the highest level of discharge from the Mississippi River, and the largest pre-sampling 7-day cumulative rainfall (Fig. 2). Studies have shown that salinity was correlated with the discharge of the nearby Mississippi River (Turner et al., 2019), and that freshwater from the Mississippi River could move into the Barataria bay through tidal inlets under easterly wind conditions (Li et al., 2011, 2021). Davis Pond Diversion discharges were consistent during our sampling days, so no obvious impact on salinity was observed. The Mississippi River discharge in the fall was low enough to have salt water from the NGOM encroach further into the basin, resulting in the highest salinities in the fall. The low rainfall and high water level at Grand Isle (close to the Barataria Pass; Fig. 2b) also could contribute to the high salinities in October.

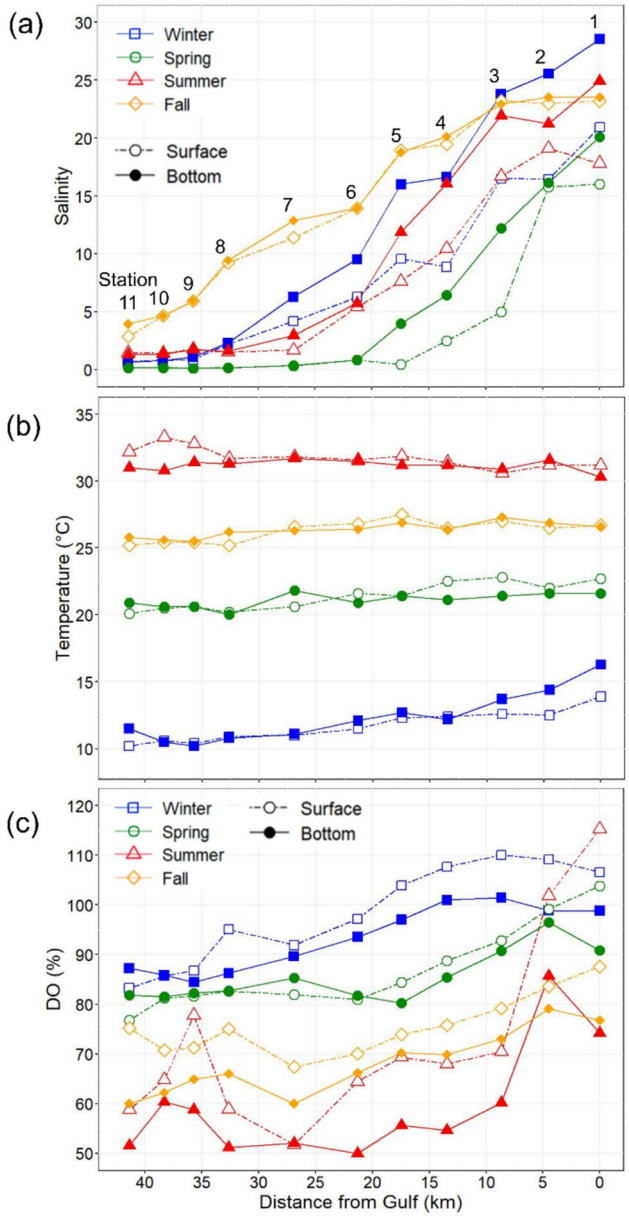

Fig. 3 Spatial and seasonal trends of surface and bottom water **a** salinity, **b** temperature, and **c** dissolved oxygen saturation (DO%) in the Barataria Basin. Different colors and shapes indicate different sampling seasons. Open shapes connected with dashed lines represent surface water samples, while solid shapes connected with solid lines represent bottom water samples

Average DO% varied seasonally between the surface and the bottom waters (Table 1; Fig. 3), with the bottom water having lower DO% than its surface counterpart at most sites. The average of the annual surface DO% was 83.2%, while the average DO% for the bottom was 76.5%. Although no sample sites reached hypoxia or anoxia, the influence of increased respiration in the water column was observed in the variance between the seasons' surface and bottom concentrations. Even though DO% excludes temperature influence in oxygen's solubility, the colder winter waters in Barataria Basin still saw the highest DO% with an average of 97.9% at the surface and 93.1% in the bottom water. The lowest DO% occurred during the summer with a surface water average of 72.8% and a bottom average of 59.5%, which coincided with increased levels of respiration associated with warm summer temperatures. The spring sampling had the least amount of variance between the surface and near bottom concentrations with a surface average of 86.7% and a bottom average of 85.4%. This was likely caused by the rainfall before sampling and associated higher winds the area received (Fig. 2). The fall surface DO% average of 75.4% was slightly greater than the bottom average of 68.0%, a slight increase from summer.

Spatiotemporal Variations of Dissolved Carbon

The DIC concentrations in the Barataria Basin varied seasonally and generally increased from the fresher sites located in the upper Barataria Basin to the Barataria Pass (Fig. 4). The DIC concentrations in the fall (average: 2588 μmol kg^{-1}) were significantly higher than the other three seasons (averages: 1685–1949 μmol kg^{-1}; Table 1; Fig. 4). Surface and

Table 1 Mean values for environmental parameters, inorganic carbon species, and nutrients in surface and bottom water samples from the four seasons of 2021. Different lowercase letters (a, b) were assigned if a statistical difference ($p < 0.05$) was found between surface and bottom samples during a certain season, while the same lowercase letter (a) indicates no statistical differences. Different uppercase letters (e.g., A, B, C) were assigned if statistical differences ($p < 0.05$) were found between seasons, while the same uppercase letter (e.g., A) indicates no statistical differences. *S* + *B* average values of surface and bottom samples

Month	Location	Salinity	Temp (°C)	DO (%)	DIC (μmol kg^{-1})	TA (μmol kg^{-1})	DIC/TA	pCO_2 (μatm)	$NO_2 + NO_3$ (μM)	PO_4 (μM)	SiO_4 (μM)
January	Surface	7.9a	11.7a	97.9a	1553a	1897a	0.81a	326	11.07a	0.07a	46.59a
Winter	Bottom	11.9a	12.3a	93.1a	2319b	2081a	1.13b	n.a	9.99a	0.07a	36.26a
	S + B	9.9AB	12.0A	95.5A	1936A	1989A	0.97A	n.a	10.53A	0.07A	41.42AB
April	Surface	3.8a	21.4a	86.7a	1627a	1217a	1.37a	718	21.81a	0.27a	38.25a
Spring	Bottom	5.5a	21.1a	85.4a	1742a	1326a	1.35a	n.a	18.79a	0.24a	38.51a
	S + B	4.6A	21.2B	86.0B	1685A	1271B	1.36BC	n.a	20.30B	0.26B	38.38AB
July	Surface	7.7a	31.8a	72.8a	1925a	1331a	1.55a	576	0.36a	0.14a	51.65a
Summer	Bottom	10.1a	31.2b	59.5b	1974a	2011a	1.39a	n.a	0.57a	0.13a	44.45a
	S + B	8.9AB	31.5C	66.2C	1949A	1671AB	1.47B	n.a	0.46C	0.14A	48.05A
October	Surface	14.2a	26.3a	75.4a	2582a	2217a	1.20a	605	0.20a	0.08a	29.82a
Fall	Bottom	14.5a	26.4a	68.0b	2593a	2338a	1.26a	n.a	0.26a	0.08a	28.37a
	S + B	14.3B	26.3D	71.7C	2588B	2278A	1.23C	n.a	0.23C	0.08A	29.09B

bottom water had similar trends, with bottom DIC usually slightly higher than surface DIC. However, surface and bottom DIC concentrations in winter were significantly different from each other, with the surface averaging 1553 μmol kg^{-1} and the bottom averaging 2319 μmol kg^{-1}.

The TA values in the Barataria Basin showed spatial and temporal trends similar to those of DIC, but with some outliers, especially for the summer and fall seasons (Fig. 4). We currently lack a definitive explanation for the four elevated TA values observed during summer and fall, which were identified as outliers in this study. However, it is plausible that anaerobic respiration processes, such as sulfate reduction—known to produce high alkalinity—may contribute via porewater exchange. Overall, TA values generally increased from station 11 (freshwater station) to station 1 (saltwater station), with mean TA at stations 11 and 1 of 1706 and 2424 μmol kg^{-1}, respectively. Even though the differences were not significant (Table 1), bottom TA values were usually higher than surface TA, with the exception of the fall season, when there were no clean trends in surface versus bottom TA. The average annual surface TA was 1922 μmol kg^{-1}, while the average TA for the bottom was 2157 μmol kg^{-1} or 235 μmol kg^{-1} higher than the surface average.

Except for the winter surface samples and a few outliers, DIC concentrations were usually higher than the corresponding TA values, leading to DIC/TA values larger than 1 (Table 1; Fig. 4). In general, DIC/TA ratios decreased from freshwater station 11 to saltwater station 1, with mean DIC/TA ratios at stations 11 and 1 of 1.5 and 0.9, respectively. Seasonally, DIC/TA ratios were the lowest in winter and the highest in summer, with DIC/TA ratios averaging 0.97 and 1.47, respectively.

Large variations in pCO_2 were observed between different seasons, all of which had increasing pCO_2 towards the freshwater endmember, with mean pCO_2 at stations 11 and 1 of 876 and 342 μatm, respectively. The five southernmost stations (1–5) had similar pCO_2 for the spring, summer, and fall seasons, while the other six stations had more seasonal variations. The winter season had the lowest pCO_2, ranging from 246 to 597 μatm, with an average of 326 μatm. The spring had the largest range overall of 342 μatm to 1192 μatm. The summer and fall seasons had similar pCO_2 values, averaging 576 and 605 μatm, respectively.

Spatiotemporal Variations of Nutrients

Concentrations of $NO_2 + NO_3$ in the Barataria Basin varied seasonally with significantly higher concentrations in the spring and winter and lower concentrations in the summer and fall (Fig. 5). Spring and winter $NO_2 + NO_3$ concentrations ranged from 8.84 to 24.6 μM and from 0.4 to 27.1 μM, averaging at 20.30 and 10.53 μM, respectively.

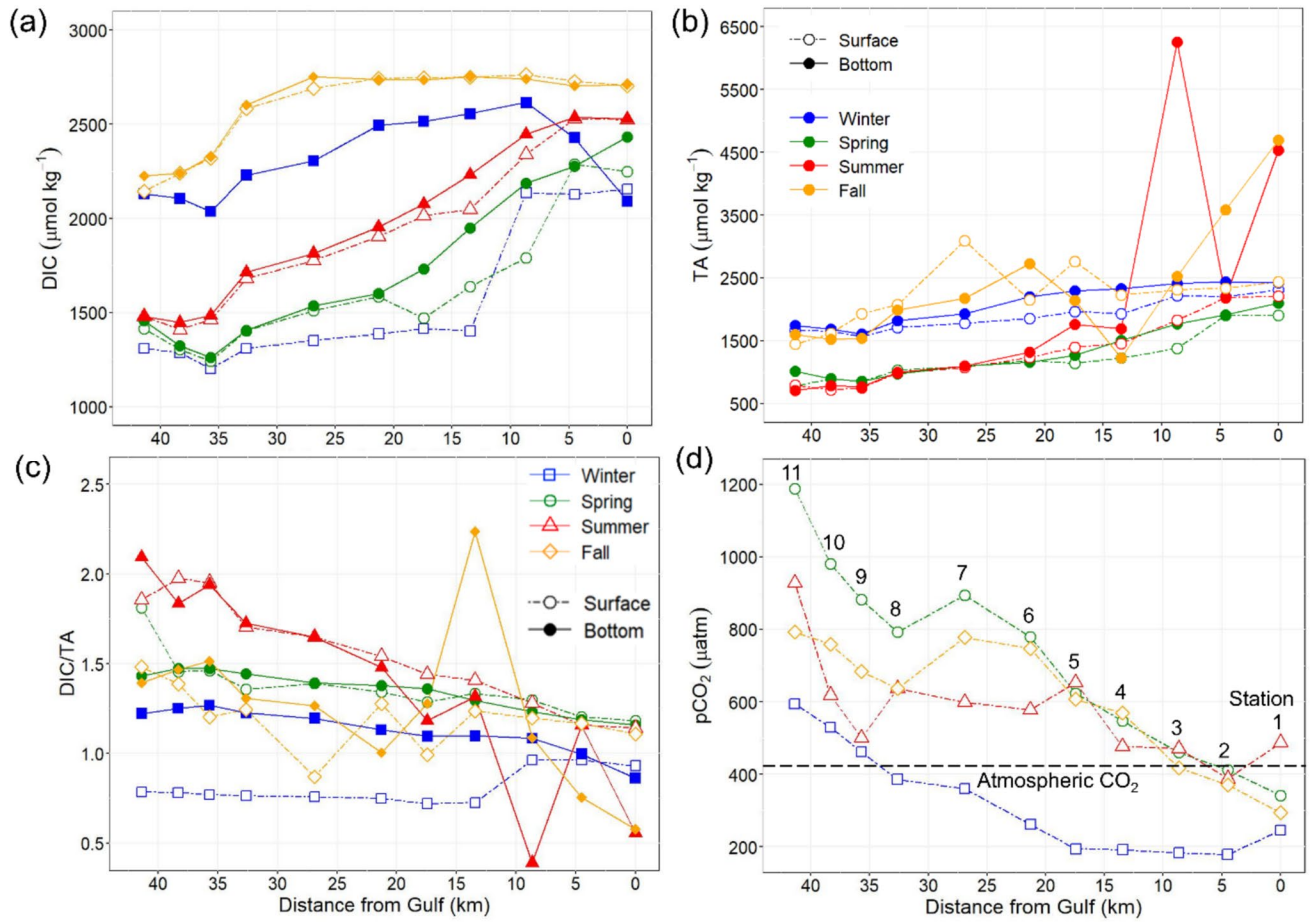

Fig. 4 Spatial and seasonal trends of surface and bottom water **a** DIC, **b** TA, **c** DIC/TA ratio, and **d** pCO_2 in the Barataria Basin. The average long-term atmospheric CO_2 collected from the coastal Louisiana buoy (28.9°N, 90.5°W) through the NOAA PMEL program is marked on panel **d** with a dashed line

Summer and fall $NO_2 + NO_3$ concentrations were two orders of magnitude lower when compared with winter and spring, averaging at only 0.46 and 0.23 µM, respectively. While the trends are not consistent across all stations, the average surface $NO_2 + NO_3$ concentrations were higher than the bottom during spring and winter and vice versa during summer and fall.

The PO_4 concentration in the Barataria Basin generally increased towards the freshwater endmember, with mean PO_4 concentrations of 0.21 and 0.05 µM at stations 11 and 1, respectively (Fig. 5). The spring season had the highest PO_4 concentrations, with an average of 0.27 µM at the surface and 0.24 µM at the bottom. In contrast to the extremely low summer $NO_2 + NO_3$ concentrations, summer PO_4 concentrations were the second highest seasonally, averaging 0.14 µM. Fall and winter PO_4 concentrations were comparable, with means of 0.079 and 0.071 µM, respectively. However, when compared with other seasons, fall PO_4 concentrations varied the least between stations, with surface and bottom PO_4 ranging 0.056–0.11 and 0.058–0.11 µM, respectively.

Concentrations of SiO_4 in the Barataria Basin varied between seasons with summer and winter having higher concentrations than spring and fall (Table 1; Fig. 5). Summer and winter SiO_4 concentrations exhibit a similar trend of increasing with distance from the Gulf of Mexico (station 1), with mean SiO_4 concentrations of 50.7 and 21.0 µM at stations 11 and 1, respectively. Surface SiO_4 concentrations were usually higher in the surface water than at the bottom, and this trend was more obvious during summer and winter seasons.

Discussion

Gulf of Mexico estuaries are dynamic coastal systems that are subject to the influences of various environmental phenomena, such as rainfall, subsequent weathering and carbonate dissolution, and evaporation, as well as physical drivers like wind and currents, which can vary with seasonality (Millero et al., 1998; Hu et al., 2017; Payandeh et al., 2019;

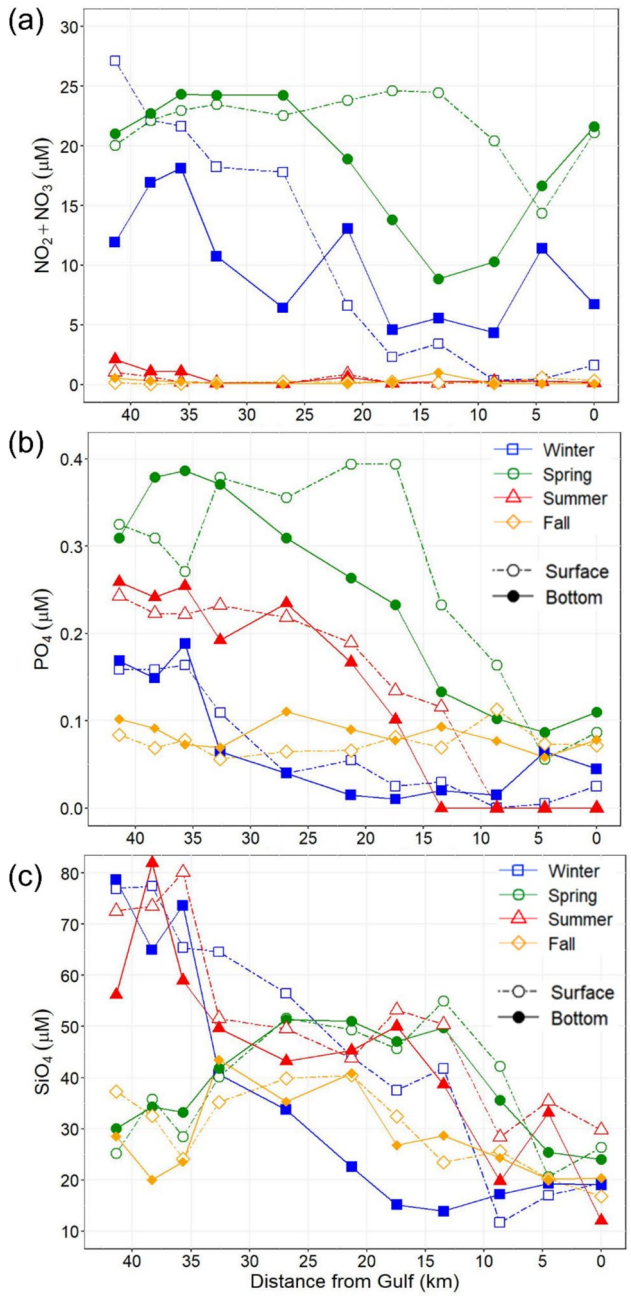

Fig. 5 Spatial and seasonal trends of surface and bottom water **a** nitrite plus nitrate (NO_2+NO_3), **b** phosphate (PO_4), and **c** silicate in the Barataria Basin

Anderson, 2020; Li et al., 2020; Sorourian et al., 2020; Hu et al., 2023). Spatial and seasonal variabilities in DIC and TA across the Barataria Basin are evident from this study. Such variabilities can be driven by a combination of sources and sinks of inorganic carbon and alkalinity into and out of the basin, especially when river alkalinity varies (Cai, 2003; Najjar et al., 2020; Stets et al., 2014; Xue & Cai, 2020). The variabilities of DIC and TA in the Barataria Basin can be largely explained by mixing caused by physical drivers, such as wind, currents, and rainfall, as well as biogeochemical processes including primary production and respiration, which both influence and are influenced by nutrient dynamics (Hu et al., 2023; Huang et al., 2021; Li et al., 2020; Payandeh et al., 2019; Ren et al., 2020; Turner et al., 2019).

The nutrient dynamics in the Barataria Basin are inherently complex. For example, the seasonal trend of SiO_4 does not match the observed NO_2+NO_3 trends, potentially due to seasonal differences in the plankton community. For spring and fall, SiO_4 concentrations first increased then decreased from stations 1 to 11, with maximum SiO_4 concentrations around stations 6 and 7. The plankton community during spring and fall is usually dominated by diatoms which prefer moderate temperatures while cyanobacteria become more abundant during summer (Bargu et al., 2016 and 2019; Matsubara et al., 2022; Turner et al., 2019). This results in larger drawdown of silica during spring and fall as indicated by low dissolved silica observed at the freshwater stations (Fig. 5c), where diatoms are more abundant because the suspended solid concentrations there were usually higher (Turner et al., 2019). Throughout this manuscript, we focus on utilizing nutrient data to analyze the spatial and seasonal trends of carbonate chemistry, as nutrient availability impacts biological productivity, which, in turn, influences carbonate chemistry.

Spatial Trend of Inorganic Carbon Chemistry

Both DIC and TA values in the Barataria Basin increased from the fresher sites located in the upper Barataria Basin to the saltier sites closer to the Barataria Pass, following the salinity pattern (Figs. 3 and 4). In freshwaters, more CO_2 outgases into the atmosphere, and less CO_2 dissociates into CO_3^{2-} and HCO_3^- due to lower solubility. As a result, TA and DIC values in freshwaters are generally lower than those in saline waters (Cai et al., 2021). Despite a decrease in pCO_2 from fresh to saline stations (Fig. 4), both DIC and TA increased with increasing salinity, consistent with trends observed in other estuaries (Brodeur et al., 2019; Yao et al., 2020). Thus, we expected to see conservative mixing play an important role in the carbonate chemistry of the Barataria Basin, similar to other estuaries (Brodeur et al., 2019; Najjar et al., 2020; Song et al., 2023; Yao et al., 2020). In order to better understand the extent of the mixing process on the DIC, TA, and pCO_2 dynamics in the basin, we constructed conservative mixing lines for surface water samples using the freshwater and saltwater endmembers (Fig. 6). Mixing analyses were performed on surface water samples only, as bottom water could be influenced by benthic fluxes. Station 11 and station 1 were used as the two endmembers of water entering our study area. The DPD is located approximately 45 km north of station 11. It is worth noting that Lake Cataouatche, the

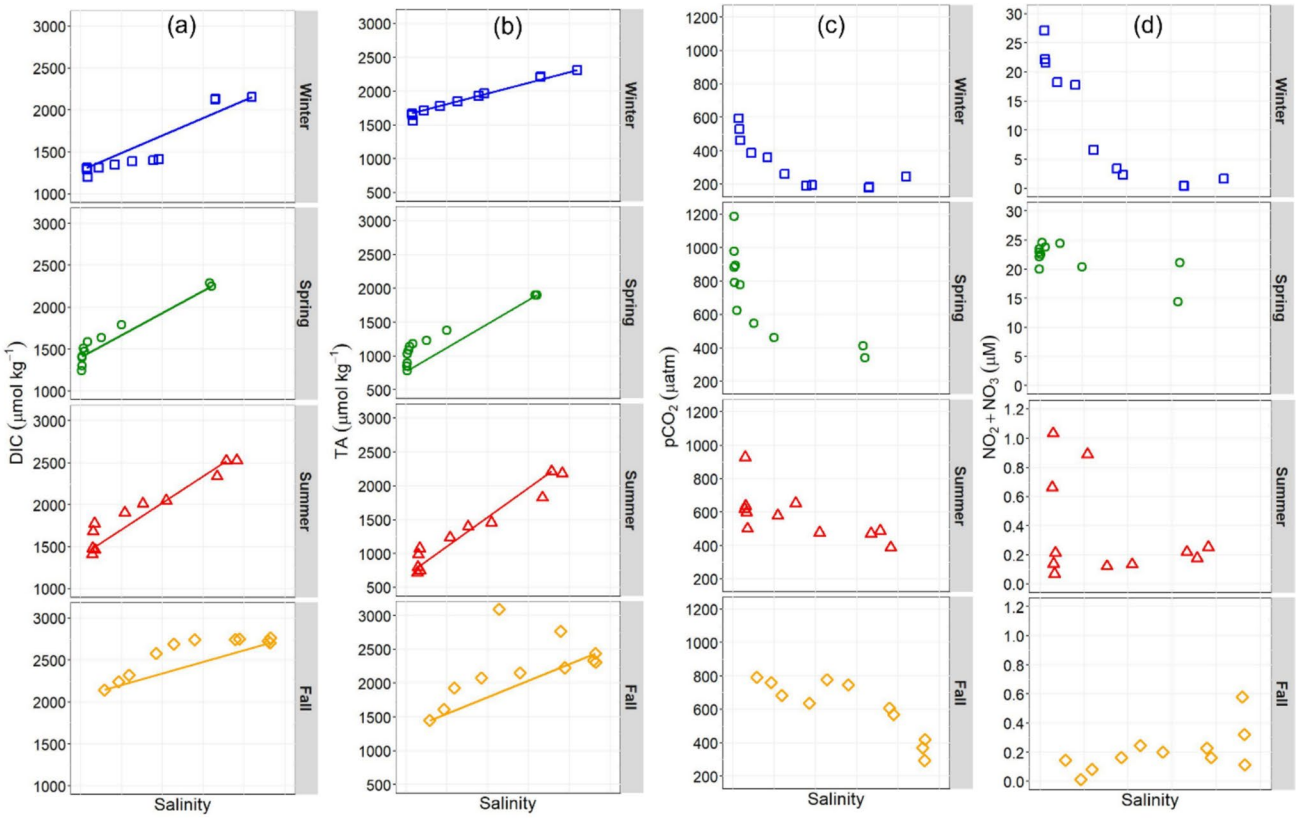

Fig. 6 Relationships between surface DIC, TA, pCO_2, $NO_2 + NO_3$ values and salinity in the Barataria Basin. Solid lines connect data from stations 1 and 11. Please note that the y-axis range for $NO_2 + NO_3$ differ among seasons

lake which the DPD directly empties into, and Lake Salvador, located directly north of the sample area, are entirely made up of freshwater habitats with minimal influence from the salt of the lower Barataria Basin (Conner & Day, 1988). On the other hand, the lower Barataria Basin (stations 1–5) is directly influenced by the Gulf of Mexico due to tidal exchanges that occur thorough the Barataria Pass and other tidal passes (Ou et al., 2020). Thus, stations 11 (the northernmost station) and 1 (the southernmost station) were used as freshwater and saltwater endmembers, respectively, to evaluate addition or removal processes within our study area when constructing conservative mixing lines. Deviations from the physical mixing lines in an estuary indicate non-conservative behavior, with values falling below the mixing lines representing removal and those above representing addition of the chemical species (Officer, 1979). The observed deviations in DIC and TA from a pure endmember mixing model can be represented as ΔDIC and ΔTA and can be utilized in conjunction with each other or DO% to better understand the combination of biogeochemical processes that are impacting carbonate chemistry (Fig. 7). At a given station, ΔDIC and ΔTA are obtained from DIC and TA at that station by subtracting the relevant conservative two-endmember mixing values calculated using stations 1 and 11.

The mixing analyses for surface DIC, TA, and pCO_2 demonstrated that while DIC and TA increased with salinity and pCO_2 decreased with salinity, all three parameters demonstrated non-conservative behavior, with the exception of TA in winter. This suggests that while conservative mixing plays an important role in the spatial trend of carbonate chemistry, other processes, such as photosynthesis and respiration, are vital to our understanding of the carbonate dynamics of this estuary. The effects of these processes are in evidence in the subsequent evaluation of the seasonal pattern in our carbonate and nutrient data.

Seasonal Pattern in Inorganic Carbon Chemistry

Winter

The DIC concentrations in winter surface water when plotted on mixing line indicate a small net DIC removal for most stations (Fig. 6a). DIC is removed from the water column during primary production and added during respiration. DIC distribution in the water represents a balance between

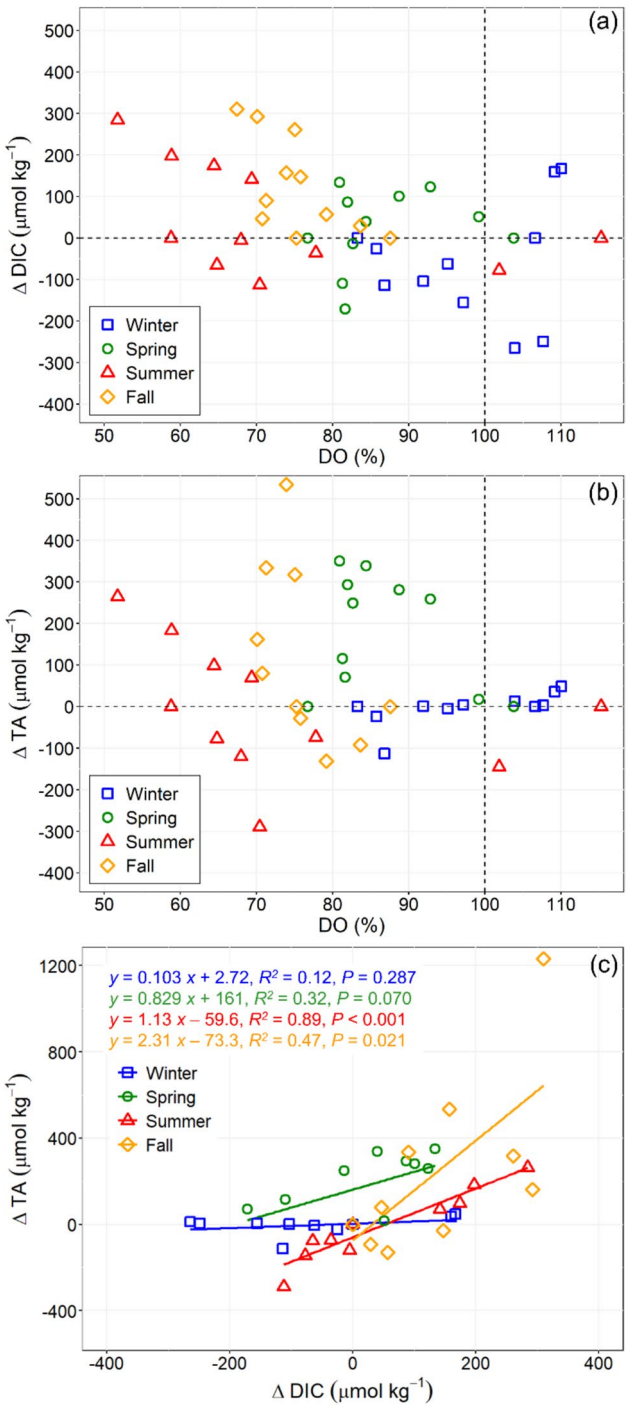

Fig. 7 Relationships between ΔDIC, ΔTA, and DO% in surface water samples in the Barataria Basin

production and respiration as well as addition or removal by other physical or chemical processes. Thus, a net DIC removal during winter suggests that production be more dominant than respiration at the surface (Sippo et al., 2016; Liu et al., 2017; Yao et al., 2020), even though winter production may not be the highest among all seasons due to low temperature (Fig. 8; Turner et al., 2019). In contrast, surface TA distribution during winter appears to be exclusively controlled by physical mixing across the transect (Fig. 6b and 7b; Huang et al., 2021). The fact that winter DIC and TA did not show a similar pattern (Fig. 6a, b) strengthens this reasoning, as primary production results in DIC drawdown with negligible change to TA (Ren et al., 2020; Sippo et al., 2016). However, primary productivity during winter is not typically high, so low respiration rates are the likely reason for observed DIC removal during this season, which could offset DIC removal through photosynthesis. Low respiration in winter is not only controlled by low temperatures but also by the reduced supply of organic matter from adjacent marshes since tidal exchange from daily flushing is limited due to low water levels (Fig. 2b). A large fraction of water column respiration is driven by the reduced supply of dissolved and particulate organic matter in winter, leading to lower DIC due to the decreased rate of remineralization and respiration (Bouillon et al., 2007; He et al., 2022).

The fact that surface productivity is more dominant than respiration during the winter season can be further explained by nutrient dynamics, as well as by surface pCO_2 patterns. Surface $NO_2 + NO_3$ concentrations experienced a sharp decrease from the fresh stations to the saline stations due to uptake by primary production, as observed in the conservative mixing analysis (Fig. 6d). The influence of primary production on PO_4 concentrations was not as distinct as on $NO_2 + NO_3$ concentrations due to the 16:1 N/P ratio in phytoplankton (Lenton & Watson, 2000). Net removal of pCO_2 was observed for the winter season even though surface water pCO_2 was lower than the atmospheric CO_2 concentration for most stations, suggesting that the removal of pCO_2 was not due to CO_2 outgassing, but due to primary productivity withdrawal.

Spring

In spring, surface water showed a small but clear deviation from conservative mixing for both DIC and TA (Fig. 6). The DIC excesses observed in the upper Barataria Basin are likely driven by enhanced water column respiration due to increased supply of organic matter from adjacent marshes and freshwater input, as well as the increase in temperature (He et al., 2022; Turner et al., 2019). Undersaturated DO values obtained for spring surface samples (Fig. 7) correspond to enhanced aerobic respiration rates, supporting this reasoning. Spring surface TA excess, however, cannot be explained by water column respiration as aerobic respiration does not produce TA. However, additional input of organic matter can contribute to TA through the addition of organic alkalinity (Song et al., 2020). Another possible explanation for TA and DIC excesses could be material exchange between the marsh and the estuary. The largest 7-day cumulative

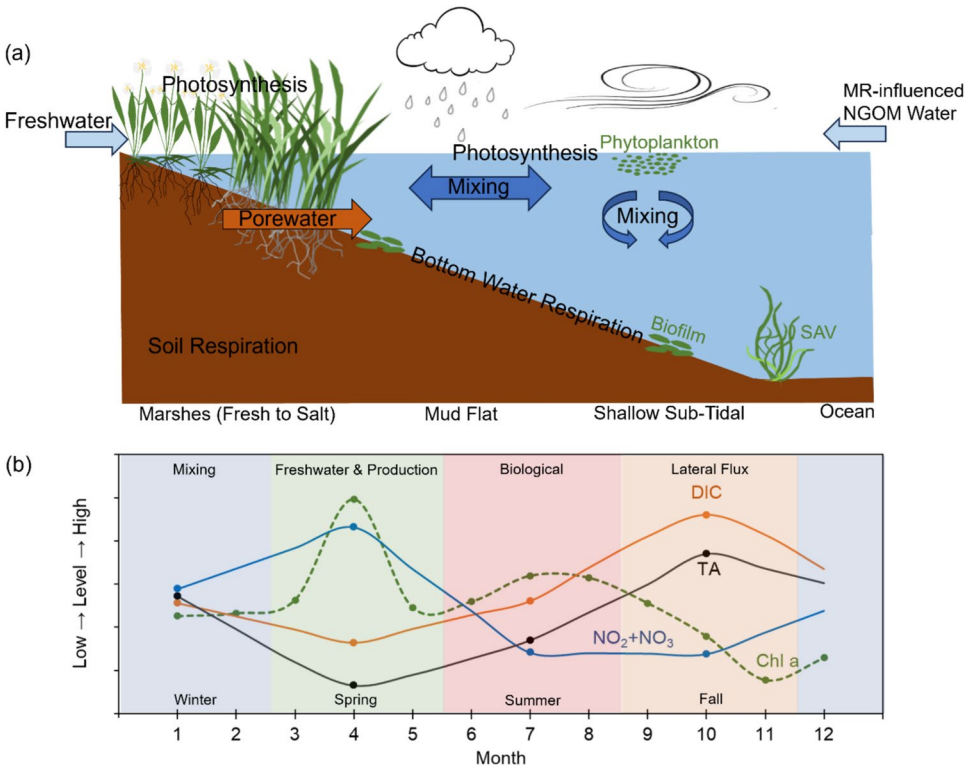

Fig. 8 The conceptual model for the carbonate system in a river-influenced shallow eutrophic estuary. Chl-a, Chlorophyll a. SAV, submerged aquatic vegetation. MR, Mississippi River. NGOM, northern Gulf of Mexico

rainfall preceding the sampling was observed in the spring (198 mm), compared to 0–10 mm during the other three seasons. Higher rainfall and freshwater discharge during this season can promote transport of marsh porewater with high DIC and TA (He et al., 2022; Reithmaier et al., 2023) to the surrounding waterbody.

The high rainfall and freshwater discharge in the spring are likely responsible for the highest seasonal NO_2+NO_3 observed during our study (Fig. 5) and resulted in the net addition of spring NO_2+NO_3 beyond mixing (Fig. 6). The large amount of rainfall before and during the spring sampling trip (Fig. 2c) could also provide NO_2+NO_3 through agricultural runoff reaching the study area from the north (Day et al., 2020; Turner et al., 2019). The strong wind from the north during spring could also facilitate runoff moving southward (Fig. 2a). High spring discharge in the Mississippi River (Fig. 2d) plays an important role in the high spring NO_2+NO_3 concentration because more Mississippi River water can potentially reach our study sites through the tidal passes in the south, bringing in high nutrient water (Li et al., 2011, 2021; Turner et al., 2019). The high NO_2+NO_3 concentrations at the northern fresh stations and in the two southern saline stations support the argument that NO_2+NO_3 enters our study area from both ends of the basin.

Nutrient dynamics in the spring can partially explain the corresponding carbonate pattern. Our results showed NO_2+NO_3 drawdown at both the surface and bottom, with bottom NO_2+NO_3 concentrations decreasing more significantly and rapidly than at the surface (Fig. 5a). Primary production occurs at the surface (phytoplankton) and at the bottom (biofilm and benthic production), which reduces both DIC and NO_2+NO_3 concentrations. Since respiration rates exceed production rates in the spring (DIC excess), the withdrawal of NO_2+NO_3 at the bottom may also be attributed to denitrification in the bottom sediment (Fig. 5a; Vaccare et al., 2019). For stations with salinity stratification (stations 1–5), our data consistently showed lower DO% and higher DIC at the bottom compared to the surface, likely due to additional benthic sediment respiration, including denitrification, in the bottom water.

Summer

The summer mixing model showed a small excess in the lower salinity range and a slight removal in the higher salinity range, indicating that surface DIC and TA were mostly controlled by conservative mixing. However, we cannot rule out the possibility that addition and removal processes were counterbalanced due to the high temperatures in summer (e.g., DIC being balanced by similar rates of respiration and photosynthesis). The small addition of both DIC and TA in the lower salinity range could reflect lateral input of respiration products from adjacent marshes, as these stations were closer to the marsh. Summer NO_2+NO_3 concentrations showed net removal and were two orders of magnitude

lower when compared with winter and spring (Figs. 5a and 6d). While primary productivity could still be very high in marshes due to high temperature leading to water column nitrate uptake, the respiration rate was likely higher than the primary production rate in the water column, as indicated by the net addition of both DIC and TA (Fig. 6). $NO_2 + NO_3$ can be removed due to marsh soil and benthic denitrification (Vaccare et al., 2019), which consumes $NO_2 + NO_3$, and produces DIC and TA. During summer, tidal marshes in the basin get tidal flushing regularly, which increases the exchange rate between the marshes and the estuary.

The small DIC and TA removal signature during summer at salinities between 10 and 20 is interesting and could be related to calcium carbonate ($CaCO_3$) precipitation by various bivalves including oysters present in the bay (Andersson & Gledhill, 2013; Sippo et al., 2016; Liu et al., 2017; Yao et al., 2020).

Fall

Surface waters in fall showed distinct DIC addition in the study area, coinciding with a similar trend in TA (Fig. 6). This concurrent increase in TA and DIC is suggestive of a similar additional source of DIC and TA, potentially a result of lateral exchange with surrounding marshes (He et al., 2022). This increase in DIC and TA through marsh porewater drainage is supported by the higher exchange rate between marsh and surface water during the fall when marshes in the Barataria Basin are flooded more frequently, partially due to higher water level in the Gulf of Mexico. This flooding can push high salinity and high DIC water from the Gulf further upstream, as shown by the higher salinities and DIC in the fall (Conner & Day, 1988; He et al., 2022; Figs. 2b, 3a, and 4a). The pCO_2 trends clearly illustrate a net removal of pCO_2 during winter, spring, and summer and a net addition in the fall (Fig. 6c). This pattern supports our conclusion that carbonate species are laterally exported in the fall through exchanges between marshes and the estuary. Our previous study (He et al., 2022) demonstrated that the DIC/TA ratios in marsh porewaters within the Barataria Basin range from 0.52 to 3.6, with an average of 1.5, and these ratios can significantly influence the ratio in adjacent water bodies. Therefore, lateral fluxes between marshes and the estuary could partially explain the high DIC/TA ratios observed in this study.

Like in summer, fall $NO_2 + NO_3$ concentrations were also extremely low compared to winter and spring (Fig. 5a). We believe that, due to high temperatures, respiration is dominant, while production is low because of the low $NO_2 + NO_3$ levels associated with decreased input of nutrient-rich freshwater (Fig. 2d).

This seasonal sampling in the Barataria Basin during 2021 revealed significant temporal variability associated with freshwater and saltwater mixing, as well as biogeochemical processes. However, the limited sampling conducted in this study makes it difficult to generalize these observations across seasons and likely provides only a snapshot of the processes dominating the system just prior to our sampling. Consequently, seasonal trends may vary annually depending on sampling timescales, and more comprehensive studies are needed to better understand the complex relationships between biogeochemical and physical processes governing the carbonate chemistry of this system. This is the first study from this region to demonstrate the extent of variability and complexity in carbonate chemistry. Overall, the limited data suggest that physical mixing plays an important role during all four seasons, with winter showing predominantly conservative mixing due to lower temperatures, which limit biological processes, and reduced water levels, which restrict lateral exchanges between the marsh and estuary. In contrast, spring, summer, and fall displayed variable impacts of biological processes and lateral exchanges with adjacent marshes. This is particularly evident in the fall, where a prominent excess of DIC and TA suggests the dominant influence of lateral fluxes of DIC and TA.

Conceptual Model and Future Trends

This seasonal study can provide a broader understanding of physical, chemical, and biological processes governing the DIC and TA distribution in eutrophic estuaries along the NGOM. The processes that impact carbonate chemistry in river-influenced shallow estuaries are summarized in Fig. 8a and represent a complex interplay between production-respiration, physical mixing processes driven by wind and tide, river discharge, and material exchanges with adjacent marshes. The seasonal variability in DIC and TA distributions within the estuary is driven by the relative contributions of these processes that vary dramatically on a temporal scale. Here, we present a seasonal conceptual model (Fig. 8b) for the Barataria Basin and similar estuaries in this region using seasonal DIC, TA, and $NO_2 + NO_3$ values collected during this study and monthly chlorophyll a data reported for a 22-year period in our study area (Turner et al., 2019;). Values of DIC, TA, and $NO_2 + NO_3$ for January, April, July, and October in Fig. 8 are the average surface and bottom DIC, TA, and $NO_2 + NO_3$ values in Table 1, while DIC, TA, and $NO_2 + NO_3$ for other months are generated using linear interpolation. Chlorophyll a data in the seasonal conceptual model are monthly means calculated using surface water chlorophyll a data collected from 1994 to 2016 for the 11 stations in our study (Turner et al., 2019). The high productivity during late spring is related to high nutrient input from the Mississippi River and runoff. $NO_2 + NO_3$ concentrations were highest during spring followed by winter and summer/fall, reflecting the influences

of the Mississippi River input and water temperature. Water temperature impacts $NO_2 + NO_3$ concentrations mostly through marsh soil denitrification and primary production in the marsh and water column, both of which consume $NO_2 + NO_3$, leading to very low $NO_2 + NO_3$ levels in summer and fall. The processes that govern nutrient supply and consumption also influence carbonate chemistry. For instance, the higher input of the Mississippi River freshwater not only added large amounts of nutrients to the system, but also decreased the DIC concentrations through drawdown via photosynthesis. However, the balance between photosynthesis and respiration cannot entirely explain the seasonal peak in DIC and TA observed during fall. We attribute this seasonal DIC and TA peak to lateral input of DIC and TA from adjacent marshes through porewater drainage. The high water level in the Gulf of Mexico (Fig. 2b) during the fall allows regular daily flushing of marsh porewater. Thus, higher porewater exchange during the fall season can contribute significantly to the DIC and TA budget because porewater tends to have lower $NO_2 + NO_3$ (denitrification) but higher DIC and TA due to high marsh soil respiration rate (He et al., 2022; Reithmaier et al., 2023).

Processes that control the carbonate and nutrient dynamics in the Barataria Basin are expected to change in the future, which adds urgency and value to our understanding of the current conditions. First, previous studies have demonstrated that changes in temperature and precipitation influence river discharge. The Mississippi River's discharge is expected to increase dramatically by the 2090s according to a process-based projection (Tao et al., 2014), which will increase the nutrient supply to the surrounding estuaries, including the Barataria Basin. Second, the Mid-Barataria Sediment Diversion, designed to combat land loss in the basin, broke ground in August 2023. This will divert up to 2100 m^3/s of fresh water from the Mississippi River directly into the Barataria Basin (CPRA 2017) and could potentially freshen saline and brackish marshes in its flow path. This influx of colder, nutrient-rich river water will not only change the salinity, but will also change marsh soil temperature, flooding regime, water residence time, and redox potential (Das et al., 2012; Hu et al., 2023; Ou et al., 2020; White et al., 2019), which in turn will change the nutrient dynamic and carbonate chemistry in the Barataria Basin (Jung et al., 2023). Our study also suggests that future changes in wind pattern and tide can also impact the carbonate budget in an estuary by influencing the water level within the semi-enclosed basin, which in turn determines the extent of material exchange with adjacent marshes.

Estuaries are uniquely sensitive to acidification as they are connection points for exchange and mixing of river water with seawater, giving rise to large vertical and horizontal gradients, which vary seasonally (Cai et al., 2021). A better understanding of nutrient dynamics and carbonate chemistry and their environmental controls is critical for predicting how future changes will impact estuaries by means of altered riverine freshwater discharge, increased water temperatures due to climate-induced warming, decreased water temperatures due to river diversions, ocean acidification, or change in the frequency and intensity of tropical storms (e.g., Jung et al., 2023; Justić et al., 1996; Ou et al., 2020; Quiñones-Rivera et al., 2022).

Conclusion

Carbonate parameters and associated nutrient values in the Barataria Basin, Louisiana, USA were investigated for the first time along spatial and temporal gradients, which will allow for better assessment and modeling of eutrophication and acidification. The aim of this study was to establish a detailed understanding of the carbonate chemistry in a dynamic, eutrophic coastal system. Such research, not previously conducted in the bays of coastal Louisiana, provides new insight on the influence of mixing and biogeochemical processes on carbonate parameters and nutrients. Our results demonstrated that while physical conservative mixing partially explains the spatial trend of carbonate parameters, the influence of biogeochemical processes deviates DIC and TA values from conservative mixing processes. Generally, in high-nutrient systems such as the Barataria Basin, seasonal carbonate chemistry is controlled by the processes that govern nutrient supply and consumption, as well as seasonal tidal flushing pattern, and porewater exchanges with adjacent marshes. The spatial carbonate trends are mostly controlled by mixing. The spatial and temporal analysis of carbonate parameters and nutrients in an estuarine environment has the potential to strengthen our understanding of the impacts of coastal biogeochemical processes on eutrophication and acidification as well as the possible vulnerabilities to acidifying conditions in the future.

Acknowledgements This work is supported by the National Science Foundation Chemical Oceanography program (award no. OCE-1756788 to Kanchan Maiti) and National Oceanic and Atmospheric Administration Sea Grant Ocean Acidification Fellowship Program. We would like to thank Eddie Weeks and Mukseet Mahmood for their help with fieldwork.

Author Contribution K.M. conceived the study design and secured funding. S.H. and S.G. completed sample collection, sample analysis, and data analysis. The initial manuscript was written by S.H. and S.G., and all authors revised and gave final approval for publication and agree to be held accountable for the work performed therein.

Data Availability The data that support the findings of this study are presented in the table and figures, and will be made available on request.

Declarations

Competing Interests The authors declare no competing interests.

References

Abril, G., Commarieu, M., Maro, D., Fontugne, M., Guérin, F., & Etcheber, H. (2004). A massive dissolved inorganic carbon release at spring tide in a highly turbid estuary. *Geophysical Research Letters* 31. https://doi.org/10.1029/2004gl019714

Anderson, M. M., Maiti, K., Xue, Z. G., & Ou, Y. (2020). Dissolved inorganic carbon transport in the surface-mixed layer of the Louisiana shelf in northern Gulf of Mexico. *Journal of Geophysical Research: Oceans* 125. https://doi.org/10.1029/2020jc016605

Andersson, A. J., & Gledhill, D. (2013). Ocean acidification and coral reefs: Effects on breakdown, dissolution, and net ecosystem calcification. *Annual Review of Marine Science, 5*, 321–348. https://doi.org/10.1146/annurev-marine-121211-172241

Bargu, S., Baustian, M. M., Rabalais, N. N., Rio, R. D., Korff, B. V., & Turner, R. E. (2016). Influence of the Mississippi River on Pseudo-nitzschia spp. Abundance and toxicity in Louisiana coastal waters. *Estuaries and Coasts, 39*, 1345–1356. https://doi.org/10.1007/s12237-016-0088-y

Bargu, S., Justic, D., White, J. R., Lane, R., Day, J., Paerl, H., & Raynie, R. (2019). Mississippi River diversions and phytoplankton dynamics in deltaic Gulf of Mexico estuaries: A review. *Estuarine, Coastal and Shelf Science, 221*, 39–52. https://doi.org/10.1016/j.ecss.2019.02.020

Bates, N., Astor, Y., Church, M., Currie, K., Dore, J., Gonaález-Dávila, M., Lorenzoni, L., Muller-Karger, F., Olafsson, J., & Santa-Casiano, M. (2014). A time-series view of changing ocean chemistry due to ocean uptake of anthropogenic CO2 and ocean acidificatiod. *Oceanography, 27*, 126–141. https://doi.org/10.5670/oceanog.2014.16

Bouillon, S., Dehairs, F., Velimirov, B., Abril, G., & Borges, A. V. (2007). Dynamics of organic and inorganic carbon across contiguous mangrove and seagrass systems (Gazi Bay, Kenya). *Journal of Geophysical Research: Biogeosciences* 112. https://doi.org/10.1029/2006jg000325.

Brodeur, J. R., Chen, B., Su, J., Xu, Y.-Y., Hussain, N., Scaboo, K. M., Zhang, Y., Testa, J. M., & Cai, W.-J. (2019). Chesapeake Bay inorganic carbon: Spatial distribution and seasonal variability. *Frontiers in Marine Science, 6*, 99. https://doi.org/10.3389/fmars.2019.00099

Cai, W.-J., Wang, Y., & Hodson, R. E. (1998). Acid-base properties of dissolved organic matter in the estuarine waters of Georgia, USA. *Geochimica Et Cosmochimica Acta, 62*, 473–483. https://doi.org/10.1016/s0016-7037(97)00363-3

Cai, W.-J., Hu, X., Huang, W.-J., Murrell, M. C., Lehrter, J. C., Lohrenz, S. E., Chou, W.-C., et al. (2011). Acidification of subsurface coastal waters enhanced by eutrophication. *Nature Geoscience, 4*, 766–770. https://doi.org/10.1038/ngeo1297

Cai, W.-J., Feely, R. A., Testa, J. M., Li, M., Evans, W., Alin, S. R., Xu, Y.-Y., et al. (2021). Natural and anthropogenic drivers of acidification in large estuaries. *Annual Review of Marine Science, 13*, 23–55. https://doi.org/10.1146/annurev-marine-010419-011004

Cai, W., Hu, X., Huang, W., Jiang, L., Wang, Y., Peng, T., & Zhang, X. (2010). Alkalinity distribution in the western North Atlantic Ocean margins. *Journal of Geophysical Research: Oceans* 115. https://doi.org/10.1029/2009jc005482

Cai, W. (2003). Riverine inorganic carbon flux and rate of biological uptake in the Mississippi River plume. *Geophysical Research Letters* 30. https://doi.org/10.1029/2002gl016312.

Conner, W. H., & Day, J. W. (1988). Rising water levels in coastal Louisiana: implications for two coastal forested wetland areas in Louisiana. *Journal of Coastal Research, 4*, 589–596. Retrieved from https://www.jstor.org/stable/4297461. Accessed 11 Feb 2025.

Couvillion, B. R., Beck, H., Schoolmaster, D., & Fischer, M. (2017). Land area change in coastal Louisiana 1932 to 2016. U.S. *Geological Survey Scientific Investigations Map, 3381*, 16. https://doi.org/10.3133/sim3381

CPRA (Coastal Protection and Restoration Authority). (2017). Louisiana's comprehensive master plan for a sustainable coast. Retrieved from http://coastal.la.gov/our-plan/2017-coastal-master-plan/. Accessed 11 Feb 2025.

Cui, L., Huang, H., Li, C., & Justic, D. (2018). Lateral circulation in a partially stratified tidal inlet. *Journal of Marine Science and Engineering, 6*, 159. https://doi.org/10.3390/jmse6040159

Das, A., Justic, D., Inoue, M., Hoda, A., Huang, H., & Park, D. (2012). Impacts of Mississippi River diversions on salinity gradients in a deltaic Louisiana estuary: Ecological and management implications. *Estuarine, Coastal and Shelf Science, 111*, 17–26. https://doi.org/10.1016/j.ecss.2012.06.005

Day, J. W., Li, B., Marx, B. D., Zhao, D., & Lane, R. R. (2020). Multivariate analyses of water quality dynamics over four decades in the Barataria Basin Mississippi Delta. *Water, 12*, 3143. https://doi.org/10.3390/w12113143

Dickson, A. (2010). Standards for ocean measurements. *Oceanography, 23*, 34–47. https://doi.org/10.5670/oceanog.2010.22

Feely, R. A., Alin, S. R., Newton, J., Sabine, C. L., Warner, M., Devol, A., Krembs, C., & Maloy, C. (2010). The combined effects of ocean acidification, mixing, and respiration on pH and carbonate saturation in an urbanized estuary. *Estuarine, Coastal and Shelf Science, 88*, 442–449. https://doi.org/10.1016/j.ecss.2010.05.004

Fitzgerald, D. M., Kulp, M., Penland, S., Flocks, J., & Kindinger, J. (2004). Morphologic and stratigraphic evolution of muddy ebb-tidal deltas along a subsiding coast: Barataria Bay, Mississippi River delta. *Sedimentology, 51*, 1157–1178. https://doi.org/10.1111/j.1365-3091.2004.00663.x

Garcia, H. E., & Gordon, L. I. (1992). Oxygen solubility in seawater: better fitting equations. *Limnology and Oceanography* 37. https://doi.org/10.4319/lo.1992.37.6.1307.

Gran, G. (1952). Determination of the equivalence point in potentiometric titrations. *Part II. Analyst, 77*, 661–671. https://doi.org/10.1039/an9527700661

He, S., Maiti, K., Swarzenski, C. M., Elsey-Quirk, T., Groseclose, G. N., & Justic, D. (2022). Porewater chemistry of Louisiana marshes with contrasting salinities and its implications for coastal acidification. *Estuarine, Coastal and Shelf Science, 268*, 107801. https://doi.org/10.1016/j.ecss.2022.107801

Hu, X., Li, Q., Huang, W.-J., Chen, B., Cai, W.-J., Rabalais, N. N., & Turner, R. E. (2017). Effects of eutrophication and benthic respiration on water column carbonate chemistry in a traditional hypoxic zone in the Northern Gulf of Mexico. *Marine Chemistry, 194*, 33–42. https://doi.org/10.1016/j.marchem.2017.04.004

Hu, K., Meselhe, E. A., & Reed, D. J. (2023). Understanding drivers of salinity and temperature dynamics in Barataria Estuary, Louisiana. *Journal of Geophysical Research: Oceans* 128. https://doi.org/10.1029/2023jc019635

Huang, W.-J., Cai, W.-J., & Hu, X. (2021). Seasonal mixing and biological controls of the carbonate system in a river-dominated continental shelf subject to eutrophication and hypoxia in the Northern Gulf of Mexico. *Frontiers in Marine Science, 8*, 621243. https://doi.org/10.3389/fmars.2021.621243

IPCC (Intergovernmental Panel on Climate Change). (2023). Summary for policymakers. In: Climate Change 2023: Synthesis Report. Contribution of Working Groups I, II and III to the Sixth Assessment Report of the Intergovernmental Panel on Climate Change [Core Writing Team, H. Lee and J. Romero (eds.)]. IPCC, Geneva, Switzerland, pp. 1–34. https://doi.org/10.59327/IPCC/AR6-9789291691647.001

Jiang, L., Cai, W., Wanninkhof, R., Wang, Y., & Lüger, H. (2008). Air-sea CO2 fluxes on the U.S. South Atlantic Bight: spatial and seasonal variability. *Journal of Geophysical Research: Oceans* 113. https://doi.org/10.1029/2007jc004366

De Jonge, V. N., Elliott, M., & Orive, E. (2002). Causes, historical development, effects and future challenges of a common environmental problem: eutrophication. Hydrobiologia, 1–19. https://doi.org/10.1023/a:1020366418295

Jung, H., Nuttle, W., Baustian, M. M., & Carruthers, T. (2023). Influence of increased freshwater inflow on nitrogen and phosphorus budgets in a dynamic subtropical estuary, Barataria Basin Louisiana. *Water, 15*, 1974. https://doi.org/10.3390/w15111974

Justić, D., Rabalais, N. N., & Turner, R. E. (1996). Effects of climate change on hypoxia in coastal waters: A doubled CO2 scenario for the northern Gulf of Mexico. *Limnology and Oceanography, 41*, 992–1003. https://doi.org/10.4319/lo.1996.41.5.0992

Kelly, R. P., Foley, M. M., Fisher, W. S., Feely, R. A., Halpern, B. S., Waldbusser, G. G., & Caldwell, M. R. (2011). Mitigating local causes of ocean acidification with existing laws. *Science, 332*, 1036–1037. https://doi.org/10.1126/science.1203815

Lenton, T. M., & Watson, A. J. (2000). Redfield revisited: 1. Regulation of nitrate, phosphate, and oxygen in the ocean. *Global Biogeochemical Cycles, 14*, 225–248. https://doi.org/10.1029/1999gb900065

Li, C., Huang, W., Wu, R., & Sheremet, A. (2020). Weather induced quasi-periodic motions in estuaries and bays: Meteorological tide. *China Ocean Engineering, 34*, 299–313. https://doi.org/10.1007/s13344-020-0028-2

Li, G., Xu, K., Xue, Z. G., Liu, H., & Bentley, S. J. (2021). Hydrodynamics and sediment dynamics in Barataria Bay, Louisiana, USA. *Estuarine, Coastal and Shelf Science, 249*, 107090. https://doi.org/10.1016/j.ecss.2020.107090

Li, C., White, J. R., Chen, C., Lin, H., Weeks, E., Galvan, K., & Bargu, S. (2011). Summertime tidal flushing of Barataria Bay: transports of water and suspended sediments. *Journal of Geophysical Research: Oceans* 116. https://doi.org/10.1029/2010jc006566

Liu, Q., Charette, M. A., Breier, C. F., Henderson, P. B., McCorkle, D. C., Martin, W., & Dai, M. (2017). Carbonate system biogeochemistry in a subterranean estuary – Waquoit Bay, USA. *Geochimica Et Cosmochimica Acta, 203*, 422–439. https://doi.org/10.1016/j.gca.2017.01.041

Matsubara, T., Shikata, T., Sakamoto, S., Ota, H., Mine, T., & Yamaguchi, M. (2022). Effects of temperature and salinity on rejuvenation of resting cells and subsequent vegetative growth of the harmful diatom Asteroplanus karianus. *Journal of Experimental Marine Biology and Ecology, 550*, 151719. https://doi.org/10.1016/j.jembe.2022.151719

Millero, F. J., Lee, K., & Roche, M. (1998). Distribution of alkalinity in the surface waters of the major oceans. *Marine Chemistry, 60*, 111–130. https://doi.org/10.1016/s0304-4203(97)00084-4

Murrell, M. C., Stanley, R. S., Lehrter, J. C., & Hagy, J. D. (2013). Plankton community respiration, net ecosystem metabolism, and oxygen dynamics on the Louisiana continental shelf: Implications for hypoxia. *Continental Shelf Research, 52*, 27–38. https://doi.org/10.1016/j.csr.2012.10.010

Najjar, R. G., Herrmann, M., Valle, S. M. C. D., Friedman, J. R., Friedrichs, M. A. M., Harris, L. A., Shadwick, E. H., Stets, E. G., & Woodland, R. J. (2020). Alkalinity in tidal tributaries of the Chesapeake Bay. *Journal of Geophysical Research: Oceans* 125. https://doi.org/10.1029/2019jc015597

Officer, C. B. (1979). Discussion of the behaviour of nonconservative dissolved constituents in estuaries. *Estuarine and Coastal Marine Science, 9*, 91–94. https://doi.org/10.1016/0302-3524(79)90009-4

Osborne, E., Hu, X., Hall, E. R., Yates, K., Vreeland-Dawson, J., Shamberger, K., Barbero, L., et al. (2022). Ocean acidification in the Gulf of Mexico: Drivers, impacts, and unknowns. *Progress in Oceanography, 209*, 102882. https://doi.org/10.1016/j.pocean.2022.102882

Ou, Y., Xue, Z. G., Li, C., Xu, K., White, J. R., Bentley, S. J., & Zang, Z. (2020). A numerical investigation of salinity variations in the Barataria Estuary, Louisiana in connection with the Mississippi River and restoration activities. *Estuarine, Coastal and Shelf Science, 245*, 107021. https://doi.org/10.1016/j.ecss.2020.107021

Payandeh, A. R., Justic, D., Mariotti, G., Huang, H., & Sorourian, S. (2019). Subtidal water level and current variability in a bar-built estuary during cold front season: Barataria Bay, Gulf of Mexico. *Journal of Geophysical Research: Oceans, 124*, 7226–7246. https://doi.org/10.1029/2019jc015081

Peyronnin, N. S., Caffey, R. H., Cowan, J. H., Justic, D., Kolker, A. S., Laska, S. B., McCorquodale, A., et al. (2017). Optimizing sediment diversion operations: Working group recommendations for integrating complex ecological and social landscape interactions. *Water, 9*, 368. https://doi.org/10.3390/w9060368

Platon, E., Gupta, B. K. S., Rabalais, N. N., & Turner, R. E. (2005). Effect of seasonal hypoxia on the benthic foraminiferal community of the Louisiana inner continental shelf: The 20th century record. *Marine Micropaleontology, 54*, 263–283. https://doi.org/10.1016/j.marmicro.2004.12.004

Quiñones-Rivera, Z. J., Wissel, B., Turner, R. E., Rabalais, N. N., Justić, D., Finlay, K. P., & Milan, C. S. (2022). Divergent effects of biological and physical processes on dissolved oxygen and dissolved inorganic carbon dynamics on a eutrophied and hypoxic continental shelf. *Limnology and Oceanography, 67*, 2603–2616. https://doi.org/10.1002/lno.12225

Rabalais, N. N., Turner, R. E., & Wiseman, W. J. (2002). Gulf of Mexico hypoxia, a.k.a. "The Dead Zone." *Annual Review of Ecology and Systematics, 33*, 235–263. https://doi.org/10.1146/annurev.ecolsys.33.010802.150513

Reithmaier, G. M. S., Cabral, A., Akhand, A., Bogard, M. J., Borges, A. V., Bouillon, S., Burdige, D. J., et al. (2023). Carbonate chemistry and carbon sequestration driven by inorganic carbon outwelling from mangroves and saltmarshes. *Nature Communications, 14*, 8196. https://doi.org/10.1038/s41467-023-44037-w

Ren, L., Rabalais, N. N., & Turner, R. E. (2020). Effects of Mississippi River water on phytoplankton growth and composition in the upper Barataria estuary, Louisiana. *Hydrobiologia, 847*, 1831–1850. https://doi.org/10.1007/s10750-020-04214-0

Sabine, C. L., Feely, R. A., Gruber, N., Key, R. M., Lee, K., Bullister, J. L., Wanninkhof, R., et al. (2004). The oceanic sink for anthropogenic CO2. *Science, 305*, 367–371. https://doi.org/10.1126/science.1097403

Salisbury, J., Green, M., Hunt, C., & Campbell, J. (2008). Coastal acidification by rivers: A threat to shellfish? *Eos, Transactions American Geophysical Union, 89*, 513–513. https://doi.org/10.1029/2008eo500001

Sarma, V. V. S. S., Kumar, N. A., Prasad, V. R., Venkataramana, V., Appalanaidu, S., Sridevi, B., Kumar, B. S. K., et al. (2011). High CO2 emissions from the tropical Godavari estuary (India) associated with monsoon river discharges. *Geophysical Research Letters* 38, n/a-n/a. https://doi.org/10.1029/2011gl046928

Schnetger, B., & Lehners, C. (2014). Determination of nitrate plus nitrite in small volume marine water samples using vanadium(III) chloride as a reduction agent. *Marine Chemistry, 160*, 91–98. https://doi.org/10.1016/j.marchem.2014.01.010

Sippo, J. Z., Maher, D. T., Tait, D. R., Holloway, C., & Santos, I. R. (2016). Are mangroves drivers or buffers of coastal acidification? Insights from alkalinity and dissolved inorganic carbon export estimates across a latitudinal transect. *Global Biogeochemical Cycles, 30*, 753–766. https://doi.org/10.1002/2015gb005324

Song, S., Wang, Z. A., Gonneea, M. E., Kroeger, K. D., Chu, S. N., Li, D., & Liang, H. (2020). An important biogeochemical link between organic and inorganic carbon cycling: Effects of organic alkalinity on carbonate chemistry in coastal waters influenced by intertidal salt marshes. *Geochimica Et Cosmochimica Acta, 275*, 123–139. https://doi.org/10.1016/j.gca.2020.02.013

Song, S., Bellerby, R., Liu, J., Guo, W., Yu, P., Ge, J., & Li, D. (2023). Impacts of an extreme Changjiang flood on variations in carbon cycle components in the Changjiang Estuary and adjacent East China sea. *Continental Shelf Research, 269*, 105137. https://doi.org/10.1016/j.csr.2023.105137

Sorourian, S., Huang, H., Li, C., Justic, D., & Payandeh, A. R. (2020). Wave dynamics near Barataria Bay tidal inlets during spring–summer time. *Ocean Modeling, 147*, 101553. https://doi.org/10.1016/j.ocemod.2019.101553

Stets, E. G., Kelly, V. J., & Crawford, C. G. (2014). Long-term trends in alkalinity in large rivers of the conterminous US in relation to acidification, agriculture, and hydrologic modification. *Science of the Total Environment, 488*, 280–289. https://doi.org/10.1016/j.scitotenv.2014.04.054

Sunda, W. G., & Cai, W.-J. (2012). Eutrophication induced CO2-acidification of subsurface coastal waters: Interactive effects of temperature, salinity, and atmospheric pCO2. *Environmental Science & Technology, 46*, 10651–10659. https://doi.org/10.1021/es300626f

Sweet, J. A., Bargu, S., Morrison, W. L., Parsons, M., Pathare, M. G., Roberts, B. J., Soniat, T. M., & Stauffer, B. A. (2022). Phytoplankton dynamics in Louisiana estuaries: Building a baseline to understand current and future change. *Marine Pollution Bulletin, 175*, 113344. https://doi.org/10.1016/j.marpolbul.2022.113344

Tao, B., Tian, H., Ren, W., Yang, J., Yang, Q., He, R., Cai, W., & Lohrenz, S. (2014). Increasing Mississippi river discharge throughout the 21st century influenced by changes in climate, land use, and atmospheric CO2. *Geophysical Research Letters, 41*, 4978–4986. https://doi.org/10.1002/2014gl060361

Turner, R. E., Swenson, E. M., Milan, C. S., & Lee, J. M. (2019). Spatial variations in chlorophyll a, C, N, and P in a Louisiana estuary from 1994 to 2016. *Hydrobiologia, 834*, 131–144. https://doi.org/10.1007/s10750-019-3918-7

Vaccare, J., Meselhe, E., & White, J. R. (2019). The denitrification potential of eroding wetlands in Barataria Bay, LA, USA: Implications for river reconnection. *Science of the Total Environment, 686*, 529–537. https://doi.org/10.1016/j.scitotenv.2019.05.475

Vargas-Lopez, I. A., Rivera-Monroy, V. H., Day, J. W., Whitbeck, J., Maiti, K., Madden, C. J., & Trasviña-Castro, A. (2021). Assessing chlorophyll a spatiotemporal patterns combining in situ continuous fluorometry measurements and Landsat 8/OLI data across the Barataria Basin (Louisiana, USA). *Water, 13*, 512. https://doi.org/10.3390/w13040512

Wang, Z. A., Kroeger, K. D., Ganju, N. K., Gonneea, M. E., & Chu, S. N. (2016). Intertidal salt marshes as an important source of inorganic carbon to the coastal ocean. *Limnology and Oceanography, 61*(5), 1916–1931. https://doi.org/10.1002/lno.10347

Wang, H., Lehrter, J., Maiti, K., Fennel, K., Laurent, A., Rabalais, N., Hussain, N., et al. (2020). Benthic respiration in hypoxic waters enhances bottom water acidification in the Northern Gulf of Mexico. *Journal of Geophysical Research: Oceans* 125. https://doi.org/10.1029/2020jc016152

White, J. R., DeLaune, R. D., Justic, D., Day, J. W., Pahl, J., Lane, R. R., Boynton, W. R., & Twilley, R. R. (2019). Consequences of Mississippi River diversions on nutrient dynamics of coastal wetland soils and estuarine sediments: A review. *Estuarine, Coastal and Shelf Science, 224*, 209–216. https://doi.org/10.1016/j.ecss.2019.04.027

Xue, L., & Cai, W.-J. (2020). Total alkalinity minus dissolved inorganic carbon as a proxy for deciphering ocean acidification mechanisms. *Marine Chemistry, 222*, 103791. https://doi.org/10.1016/j.marchem.2020.103791

Xue, Z., He, R., Fennel, K., Cai, W.-J., Lohrenz, S., Huang, W.-J., Tian, H., Ren, W., & Zang, Z. (2016). Modeling pCO2 variability in the Gulf of Mexico. *Biogeosciences, 13*, 4359–4377. https://doi.org/10.5194/bg-13-4359-2016

Yao, H., McCutcheon, M. R., Staryk, C. J., & Hu, X. (2020). Hydrologic controls on CO2 chemistry and flux in subtropical lagoonal estuaries of the northwestern Gulf of Mexico. *Limnology and Oceanography, 65*, 1380–1398. https://doi.org/10.1002/lno.11394